UNIVERSITY
OF
QUEENSLAND

Department of Civil Engineering

RESEARCH REPORT SERIES

The Analysis of Thermal Stress Involving Non-Linear Material Behaviour

. BEER and J.L. MEEK

esearch Report No. CE10
April, 1980

CIVIL ENGINEERING RESEARCH REPORTS

This report is one of a continuing series of Research Reports published by the Department of Civil Engineering at the University of Queensland. This Department also publishes a continuing series of Bulletins. Lists of recently published titles in both of these series are provided inside the back cover of this report. Requests for copies of any of these documents should be addressed to the Departmental Secretary.

The interpretations and opinions expressed herein are solely those of the author(s). Considerable care has been taken to ensure the accuracy of the material presented. Nevertheless, responsibility for the use of this material rests with the user.

Department of Civil Engineering,
University of Queensland,
St Lucia, Q 4067, Australia,
[Tel:(07) 377-3342, Telex:UNIVQLD AA40315]

THE ANALYSIS OF THERMAL STRESS INVOLVING NON-LINEAR MATERIAL BEHAVIOUR

by

G. Beer, Dip Ing *Austria*, M Sc *Lehigh*, PhD, MIE Aust.
Senior Research Assistant

and

J. L. Meek, MS *Calif.*, BE, BSc, PhD
Reader in Civil Engineering

RESEARCH REPORT NO. CE 10
Department of Civil Engineering
University of Queensland

Synopsis

The research sets out to solve two non-linear analyses problems, namely the transient heat phenomena due to welding and the subsequent elasto-plastic stress analysis. Both analyses employ the finite element method and it is assumed that the termperature distribution can be calculated independent from the stress analysis. Von-Mises plasticity is used with variation of material properties with temperature. Results are presented for the effect of a weld line across the edge of a flat plate and the residual stresses compared with experimental values.

CONTENTS

1. INTRODUCTION

The analysis presented in this paper is an application of the finite element method in the prediction of non-linear material behaviour of continuum type structures. The particular continuum chosen for analysis is that of plane-stress or strain, composed of a material whose yield stress may be predicted by the Von-Mises - Hencky criterion. The non-linear effects chosen for investigation are those resulting from high-temperatures, such as welding. The problem thus involves two stages of analysis. The first stage requires the solution to the non-linear transient heat flow problem in which the heat source varies in position with time. The thermal properties are assumed to be independent of any induced stress. From this analysis, termperature strains are calculated at each time interval and these used in the second stage of the analysis to predict the elasto-plastic stress distribution. Finally, when the structure has returned to the ambient temperature the pattern of residual stresses is obtained. The thermal stress analysis is complicated by change in both modulus of elasticity and yield surface with temperature. The analysis should have application in problems of residual stress determination and in determining pre-heat necessary to reduce these stresses in welding processes. For example, the effects of residual stresses from welding have been found to influence buckling behaviour of struts and plates (1).

2. THEORY OF DETERMINATION OF THERMAL STRAINS AND STRESSES

Temperature change produces change in volume. The thermal expansion from a given state is proportional to the temperature change dT and the thermal strain is given,

$$d\varepsilon_T = \alpha_T \, dT \qquad (1)$$

Of course, the coefficient of thermal expansion α_T may be a function of the temperature T, so that Equation 1 can be regarded as a tangential or incremental relationship. Thermal stresses develop when the expansion is restrained. The restraint arises because the system is statically indeterminate, either

externally with regard to its support system or internally because the non-uniform expansion inside the solid violates the compatibility requirements of strains and displacements. Fortunately, for most practical applications envisaged herein, the temperature field may be obtained independently from the stress field. That is, the heat equilibrium in the solid is not influenced by the force equilibrium or vice versa.

In this paper the emphasis is placed on stage two of the analysis, the thermo-elasto-plastic stress problem. The transient heat flow solution including high temperatures has been presented elsewhere (Refs. 2 and 3).

2.1 Constitutive Equations

For a linear elastic material, the stress change in the time interval in which the temperature changes by an amount ΔT is,

$$\{\Delta\sigma\}=[D]\ \{\Delta\varepsilon_e\} \tag{2}$$

In Equation 2, [D] is the constitutive matrix and $\{\Delta\varepsilon_e\}$, the elastic strains,

$$\{\Delta\varepsilon_e\} = \{\Delta\varepsilon\} - \{\Delta\varepsilon_T\} \tag{3}$$

The thermal strain for the increment is calculated,

$$\{\Delta\varepsilon\} = \int_0^{\Delta T} \alpha_T \, dT \tag{4}$$

The total strain change $\{\Delta\varepsilon\}$ may be approximated,

$$\{\Delta\varepsilon\} = \{\varepsilon_+\} - \{\varepsilon_-\} \tag{5}$$

There are three types of material non-linear behaviour to be considered and these are discussed separately.

2.2 Variable Elasticity

The elastic properties (E, ν) are functions of temper-

ature. Thus the elastic constitutive matrix $[D_-]$ at the beginning of the interval and $[D_+]$ at the end may differ appreciably. The stress change for the increment is,

$$\{\Delta\sigma\} = [D_+]\ \{\varepsilon_+\} - [D_-]\ \{\varepsilon_-\} \tag{6}$$

The change in the elastic constitutive matrix is,

$$[\Delta D] = [D_+] - [D_-] \tag{7}$$

with this notation, Equation 6 is written

$$\{\Delta\sigma\} = [D_+]\ \{\Delta\varepsilon\} + [\Delta D]\ \{\varepsilon_-\} \tag{8}$$

That is,

$$\{\Delta\sigma\} = [D_+]\ \left(\{\Delta\varepsilon\} - [D_+]^{-1}\ [\Delta D]\ \{\varepsilon_-\}\right) \tag{9}$$

Finally,

$$\{\Delta\sigma\} = [D_+]\ \left(\{\Delta\varepsilon\} - \{\Delta\varepsilon_{\Delta E}\}\right) \tag{10}$$

The term $\{\varepsilon_{\Delta E}\}$ in Equation 10 is called a 'pseudo' strain increment. From Equations 9 and 10, it is seen that,

$$\{\Delta\varepsilon_{\Delta E}\} = [D_+]^{-1}\ [\ D]\ \{\varepsilon_-\} \tag{11}$$

2.3 Plasticity

Plastic strains occur when the stresses at a point reach the yield surface. Irreversible plastic strains $\{\Delta\varepsilon_p\}$ occur, and,

$$\{\Delta\sigma\} = [D]\ \left(\{\Delta\varepsilon\} - \{\Delta\varepsilon_p\}\right) \tag{12}$$

The magnitude and direction of the plastic strain increments depend on the yield condition and the flow law. Herein, the Von Mises - Hencky yield condition has been used and this assumes that the yield function F is defined by the second invariant of the deviatoric stress tensor.

The condition is written,

$$F = \sigma - \sigma_y = 0 \tag{13}$$

The yield stress σ_y is obtained from a uni-axial tension test and is a function of temperature. The equivalent stress $\bar{\sigma}$ is given from the second invariant of the deviatoric stress tensor to be,

$$\bar{\sigma}^2 = \frac{3}{2} \{\sigma_D\}^T \{\sigma_D\} \tag{14}$$

In equation 14, for the three dimensional stress state,

$$\{\sigma_D\}^T = \{S_x, S_y, S_z, \sqrt{2}\,\tau_{xy}, \sqrt{2}\,\tau_{yz}, \sqrt{2}\,\tau_{zx}\} \tag{15}$$

Subsequent yield surfaces F depend on temperature and the amount of plastic strain $\{\varepsilon_p\}$ that has taken place, so that Equation 13 is written in the general form,

$$F(\bar{\sigma}_p, \bar{\varepsilon}_p, T) = 0 \tag{16}$$

Corresponding to the equivalent stress, $\bar{\sigma}$, the equivalent plastic strain $\bar{\varepsilon}_p$ is defined,

$$\bar{\varepsilon}_p^2 = \frac{2}{3} \{\varepsilon_p\}^T \{\varepsilon\} \tag{17}$$

where,

$$\{\bar{\varepsilon}_p\}^T = \{e_x, e_y, e_z, \frac{1}{\sqrt{2}}\gamma_{xy}, \frac{1}{\sqrt{2}}\gamma_{zy}, \frac{1}{\sqrt{2}}\gamma_{zx}\} \tag{18}$$

For isotropic hardening, the yield surface becomes,

$$F = \bar{\sigma} - \sigma_y (\bar{\varepsilon}_p, T) = 0 \tag{19}$$

The direction of the plastic strain increments is governed by the flow rule assumed. The Prandtl - Reuss Rule assumes that no volume change occurs during plastic straining and hence the plastic strains are dependent on the deviatoric stresses. That is, on the normal to the yield surface.

$$d\{\varepsilon_p\} = \frac{\partial F}{\partial \{\sigma\}} d\bar{\varepsilon}_p = \{S\} d\bar{\varepsilon}_p \tag{20}$$

In Equation 20,

$$\{S\}^T = \frac{2}{3} \frac{1}{\bar{\sigma}} \sigma_D \tag{21}$$

In an initial stress approach, an elastic analysis is carried out at every time increment and any plastic strains which may have occurred computed at the end of the increment.

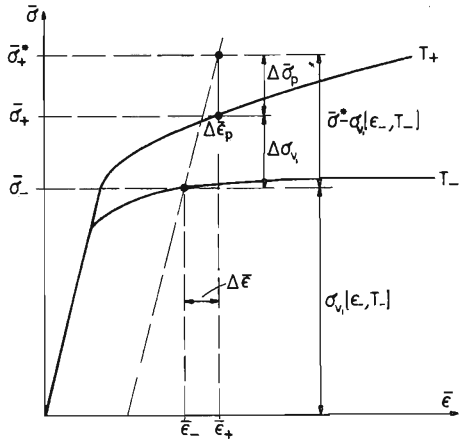

FIGURE 1 : Stress-Strain Relationships

Thus referring to Figure 1, the stress level at the end of the increment $\{\bar{\sigma}_+^*\}$ may violate the yield condition. The equivalent plastic strain increment $\Delta\bar{\varepsilon}_p$ is related to the 'elastic overstress', $\Delta\bar{\sigma}_p$, by

$$\Delta\bar{\sigma}_p = C\Delta\bar{\varepsilon}_p \tag{22}$$

The constant C has to be determined.

For small increments of $\Delta\bar{\sigma}_p$,

$$\Delta\bar{\sigma}_p = \left(\frac{\partial\sigma}{\partial\{\sigma\}}\right)^T \{\Delta\sigma_p\} = \{S\}^T \{\Delta\sigma_p\} \tag{23}$$

Also, since $\Delta\sigma_p$ is the 'elastic overstress',

$$\{\Delta\sigma_p\} = [D] \{\Delta\varepsilon_p\} \tag{24}$$

Hence, with the use of Equation 20,

$$\Delta\bar{\sigma}_p = \{S\}^T [D] \{S\} \Delta\bar{\varepsilon}_p \tag{25}$$

That is, $C = \{S\}^T [D] \{S\}$ (26)

From Figure 1, it is seen that

$$\bar{\sigma}^* - \sigma_y(\varepsilon_-, T_-) = \Delta\bar{\sigma}_p + \Delta\sigma_y \tag{27}$$

With a linear approximation of,

$$\Delta\sigma_y = \Delta\sigma_{yT} + \Delta\sigma_{yE} \tag{28}$$

Where,

$$\Delta\sigma_{yE} = \frac{\partial\sigma_y}{\partial\bar{\varepsilon}_p} \Delta\bar{\varepsilon}_p = H(T_-, \varepsilon_-) \Delta\bar{\varepsilon}_p \tag{29}$$

and,

$$\Delta\sigma_{yT} = \frac{\partial\sigma_y}{\partial T} \quad T = A(T_-, \varepsilon_-) \Delta T \tag{30}$$

In Equations 29, 30, H and A are functions of the temperature and plastic strain and may be considered as the rate of expansion of the yield surface with strain (strain hardening) and temperature respectively. Equation 27 may be now rewritten as,

$$\bar{\sigma}^* - \sigma_y(\varepsilon_-, T_-) = C\Delta\bar{\varepsilon}_p + H\Delta\bar{\varepsilon}_p + A\Delta T \tag{31}$$

Solving for $\Delta\bar{\varepsilon}_p$,

$$\Delta\bar{\varepsilon}_p = \frac{\bar{\sigma}^* - \sigma_y(\varepsilon_-, T_-) - A\Delta T}{H + C} \tag{32}$$

Then with Equation 20,

$$\{\Delta\varepsilon_p\} = \{S\}\ \Delta\bar{\varepsilon}_p \tag{33}$$

The above relationships are only approximate and for large plastic strain increments the corrected stress level may not lie on the yield surface. In such a case the above process is modified slightly and an incremental correction method based on the above is used to ensure that the final stress does lie close to the yield surface (See Appendix A).

2.4 Creep

Creep occurs when the strain at a given stress level changes with time. In general there is a coupling between creep and plastic strains. For most practical purposes, however, the creep strain may be isolated from the plastic strains. The nature of the creep strains is very similar to that of the plastic strains and hence the direction of the creep strains is obtained by using the same flow rule. That is,

$$\{\Delta\varepsilon_c\} = \{S\}\ \Delta\bar{\varepsilon}_c \tag{34}$$

Here, $\Delta\bar{\varepsilon}_c$ is the equivalent creep strain increment and establishes the relationship between the multi-axial and uni-axial stress states. Within the increment $\Delta\bar{\varepsilon}_c$ is obtained from the average creep rate inside the increment,

$$\Delta\bar{\varepsilon}_c = \dot{\varepsilon}_e \Delta t \tag{35}$$

The creep rate $\dot{\varepsilon}_c$ is dependent on the state of stress, the temperature and the accumulated creep strain or time, so that it is possible to write,

$$\dot{\varepsilon}_c = \dot{\varepsilon}_c\ (\bar{\sigma},\ T,\ \bar{\varepsilon}_{c\ \text{or}\ t}) \tag{36}$$

Several mathematical models for creep have been proposed (see Ref. 4). The stress increment for creep alone operative becomes,

$$\{\Delta\sigma\} = [D]\ (\{\Delta\varepsilon\} - \{\Delta\varepsilon_e\}) \tag{37}$$

In general all the abovementioned material non-linearities may be present and together,

$$\{\Delta\sigma\} = [D_+]\ (\{\Delta\varepsilon\} - \{\Delta\varepsilon_{\Delta E}\} - \{\Delta\varepsilon_p\} - \{\Delta\varepsilon_c\} \tag{38}$$

3. NUMERICAL IMPLEMENTATION

The above theory is incorporated in a finite element program using an 8 node isoparametric element as the basic two-dimensional block. Details of the iterative scheme used are discussed herein.

For pure thermal stress problems (no external loading), the following system of linear equations is obtained for the equilibrium at the end of a time increment.

$$[K]\ \{\Delta\delta\} = \{\Delta F_o\} \tag{39}$$

The stiffness matrix is the global assemblage of individual element stiffness matrices.

$$[k] = \int_{vol} [B]^T\ [D]\ [B]\ dV \tag{40}$$

and the initial nodal point force vector is obtained from all element contributions,

$$[\Delta f_o] = \int_{vol} [B]^T\ [D]\ \{\Delta\varepsilon_o\}\ dV \tag{41}$$

In Equation 41, $\{\Delta\varepsilon_o\}$ is the initial strain vector and contains all strains that are not stress induced or elastic. For an elastic thermal stress analysis $\{\Delta\varepsilon_o\}$ contains only the thermal strains $\{\Delta\varepsilon_T\}$. For a non-linear analysis all the non-linear effects may be considered as initial strains and hence,

$$\{\Delta\varepsilon_o\} = \{\Delta\varepsilon_{\Delta E}\} + \{\Delta\varepsilon_p\} + \{\Delta\varepsilon_c\} + \{\Delta\varepsilon_T\} \tag{42}$$

Since the magnitudes of $\{\Delta\varepsilon_p\}$ and $\{\Delta\varepsilon_c\}$ are not known at the beginning of the interval but depend on the state of stress at the end of the increment, an iterative solution is used to solve the equilibrium equations. A linear elastic analysis is carried out at the beginning with assumed values of $\{\Delta\varepsilon_p\}$ and $\{\Delta\varepsilon_c\}$, and a first approximation to the displacement increment obtained. The total strain increment is then computed, for the ith iteration,

$$\{\Delta\varepsilon_i\} = [B]\ \{\Delta\delta_i\} \tag{43}$$

The corresponding stress increment is then,

$$\{\Delta\sigma_i\} + [D]\ (\{\Delta\varepsilon_i\} - \{\Delta\varepsilon_T\} - \{\Delta\varepsilon_{\Delta E}\} - \{\Delta\varepsilon_{pi-1}\} - \{\Delta\varepsilon_{ci-1}\} \tag{44}$$

The approximation to the stress level at the end of the increment is

$$\{\sigma_{+i}\} = \{\sigma_-\} + \{\Delta\sigma_i\} \tag{45}$$

With this new stress level improved values of the plastic strain increment $\{\Delta\varepsilon_{pi}\}$ and the creep strain increment $\{\Delta\varepsilon_{ci}\}$ are computed.

The nodal point force vector is then recomputed with new values of $\{\Delta\varepsilon_p\}$ and $\{\Delta\varepsilon_c\}$

$$\{\Delta f_i\} = \int_{vol} [B]^T\ [D]\ (\{\Delta\varepsilon_T\} + \{\Delta\varepsilon_{\Delta E}\} + \{\Delta\varepsilon_{pi}\} + \{\Delta\varepsilon_{ci}\})\ dV \tag{46}$$

An improved approximation to the nodal displacement increment is made,

$$\{\Delta\delta_{i+1}\} = [K]\ \{\Delta F_i\} \tag{47}$$

The process is repeated until the 'residual force' vector

$$\{\Delta R_i\} = \{\Delta F_{i+1}\} - \{\Delta F_i\} \tag{48}$$

is small. That is, until

$$||\{\Delta R_i\}|| < \text{Tolerance limit} \tag{49}$$

The Tolerance limit is set by the user.

The method described above is referred to in the literature as the 'initial force' method. The stiffness matrix is computed with the elastic properties and in the case of variable elasticity can change throughout the loading histroy. To avoid recomputation at every time step, the changes may be moved to the right-hand side and included in the iteration process. Thus, the stiffness matrix at any time is,

$$[K] = [K_o] + [\Delta K] \tag{50}$$

Thence,

$$([K_o] + [\Delta K])\ \{\Delta \delta_i\} = \{\Delta F_{i-1}\} \tag{51}$$

and approximately for the ith iteration,

$$[K_o]\ \{\Delta \delta_i\} = \{\Delta F_{i-1}\} - [\Delta K_{i-1}]\ \{\Delta \delta_{i-1}\} \tag{52}$$

Then only the elastic stiffness matrix $[K_o]$ at room temperature occurs on the left hand side of the equations and the method is now a true 'constant stiffness' approach. The merits of a 'tangent stiffness' approach with recomputation of the stiffness at the beginning of each time interval versus a 'constant stiffness' approach have been discussed in the literature (Ref. 5). The authors have found the above process quite economical in the problems they have investigated.

Several devices may be used to accelerate convergence of the iterations, namely,

(a) A good initial assumption of $\{\Delta\varepsilon_p\}$ and $\{\Delta\varepsilon_c\}$. Where progressive plasticity occurs the starting values may be taken from the previous time increment. For cyclic plasticity any such assumption may, however, increase the number of iterations and a zero starting value for $\{\Delta\varepsilon_p\}$ would be more appropriate.

(b) The use of an over-relaxation factor where the plastic strain estimate is magnified,

$$\{\Delta\varepsilon^*_p\} = \alpha\{\Delta\varepsilon_p\} \tag{53}$$

For α values between 1.8 - 2.0, improved convergence has resulted for the case of progressive plasticity. However, for cyclic plasticity unstable oscillations may occur.

The merits of higher order isoparametric elements for the thermal stress computation and the use of numerical integration has been discussed in Ref. 6. In Ref. 6 it has also been shown that the element used for thermal stress analysis should be able to represent at least a linear distribution of strain. Thus the choice of the 8 node - 'parabolic' isoparametric element in the studies presented herein.

4. EXAMPLES

Two examples are given to demonstrate the use of the theory. In both examples the material used is structural steel and its behaviour at elevated temperatures is given as plots of stress versus strain in Fig. 2. These have been taken from test results reported in Ref. 8. The necessary information extracted from these curves is the temperature dependence of the modulus of elasticity, the strain hardening parameter H, and the change in yield stress parameter A.

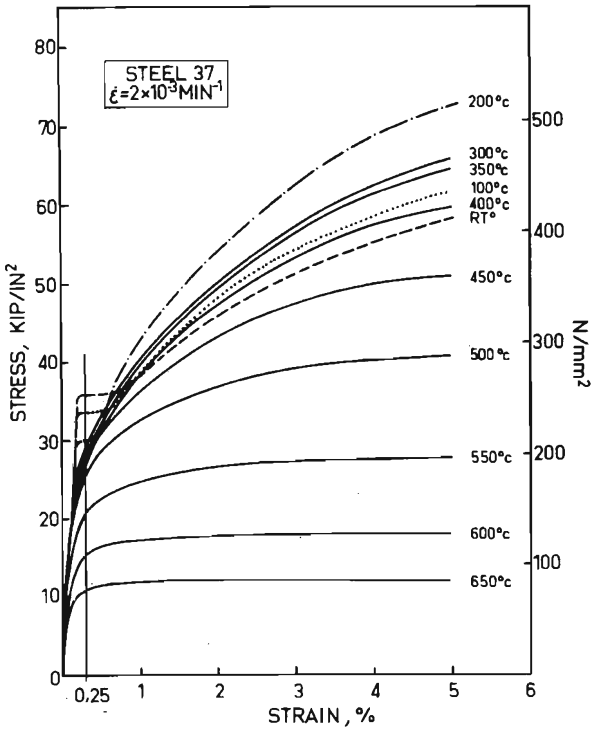

FIGURE 2 : Steel- Stress-Strain Curves
for Various Temperatures

In Fig. 3, the dependence of the modulus of elasticity on temperature is shown and a smooth function is passed through the band of available data. An accurate functional representation for A and H is very difficult if not impossible to obtain. A relatively simple function which can be used is reported in Ref. 9. For thermal stress problems discussed herein it has been assumed that the strain hardening range can be neglected with the introduction of large errors. A simple function of temperature only is used to represent σ_y and thus A. This function is shown in Fig. 4, and has been used in the examples analysed herein.

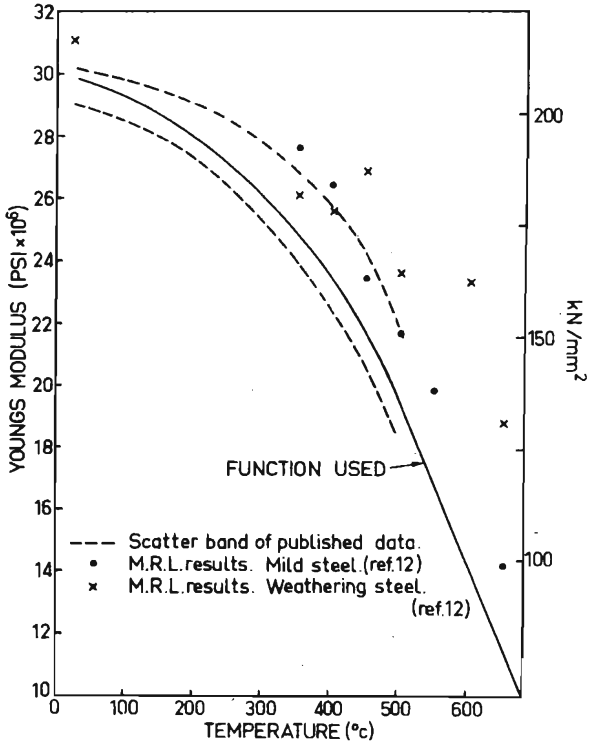

FIGURE 3 : Variation of Young's Modulus of Steel with Temperature

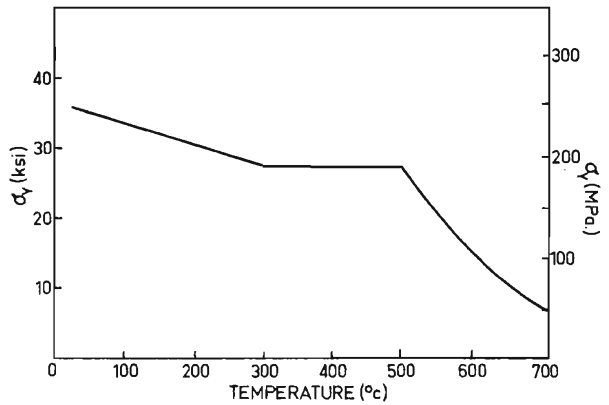

FIGURE 4 : Variation of Yield Strength of Steel with Temperature

Example 1: Thick Cylinder subjected to a temperature difference between the inside and outside surface.

The ratio of inner to external radius has been chosen to agree with that given in an analytical solution in Ref. 11. In Ref. 11, the external temperature is increased to 425°C whereas the internal temperature is constant at 0°C. The Tresca yeild criterion is used and perfect plasticity and constant material properties assumed. A comparison of this solution with the finite element analyses undertaken herein in shown in Figs. 5 and 6.

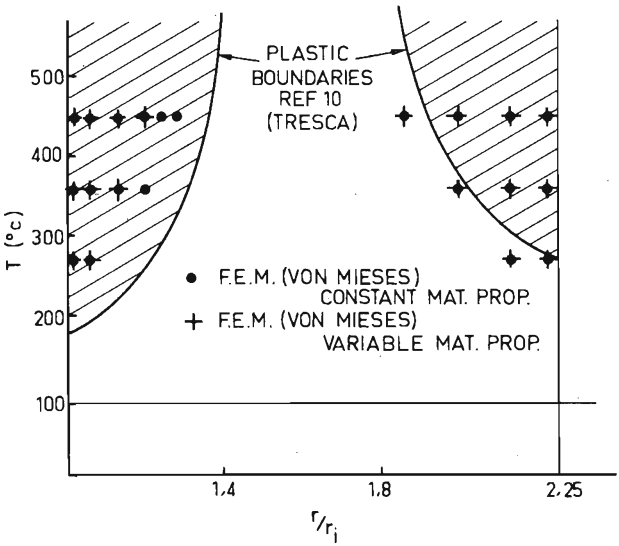

FIGURE 5 : Plastic Zones in Thick Cylinder Subject to Temperature Difference

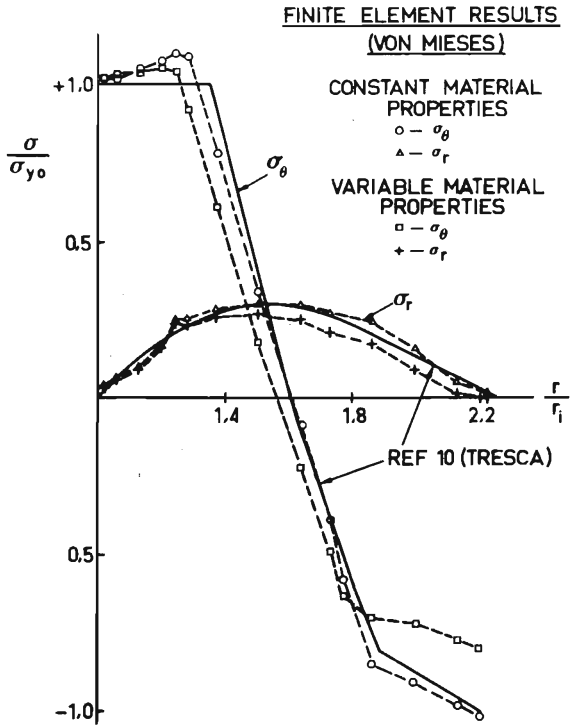

FIGURE 6 : Results of Stress Analysis of Thick Cylinder

The finite element mesh consisting of 3 elements is shown in Fig. 7. In Fig. 5 the comparison of stress distributions is given, whereas in Fig. 6, the plastic zones are shown. The results compare favourably considering the limited number of elements used and the slightly different yield criterion. A consideration of the variation of material properties with temperature causes a decrease in stresses at the hotter outside.

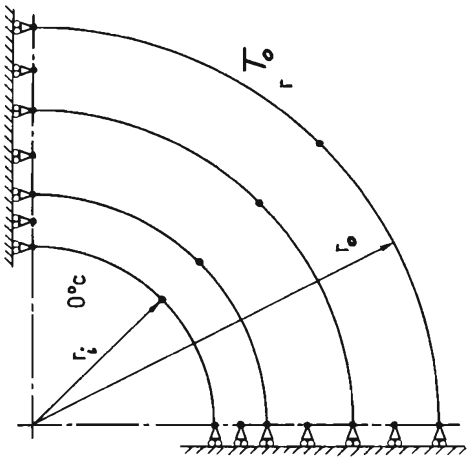

FIGURE 7 : Finite Element Mesh for Thick Cylinder

Example 2: In this second example the welding of a thin plate along one of its free edges is analysed. The welding rod is here idealized as a point heat source and the actual deposit of weld material is not considered. That is, its mass is considered small when compared with the mass of the plate. For the thin plate the simplified assumption is made for the thermal analysis that heat flow can be treated as two dimensional with no temperature variation through the thickness. The heat flow analysis was discussed in Ref. 12, and results of this shown in Fig. 9, for the finite element mesh in Fig. 8.

The results in Fig. 9 are contour plots for different times and location of the heat source (welding rod). The thermal stress analysis was performed using the high temperature material properties discussed previously. The functions for E and σ_y were extended to give zero values at the melting point (1400°C) to allow for the high temperatures encountered near the welding rod. Creep strains were not considered. The iteration process discussed previously has proved to be stable even in the extreme case where part of an element has zero strength. The same finite

element mesh shown in Fig. 8 was used in the stress analysis. In all 16 time steps were used to cover the range from beginning of welding to the complete cooling of the plate.

Within each time step a maximum of 5 iterations gave an average convergence of about 1%. The step by step computation of the plastic strain increments as discussed in Appendix A ensured that the stresses were on or very near the yield surface wherever plasticity occurred.

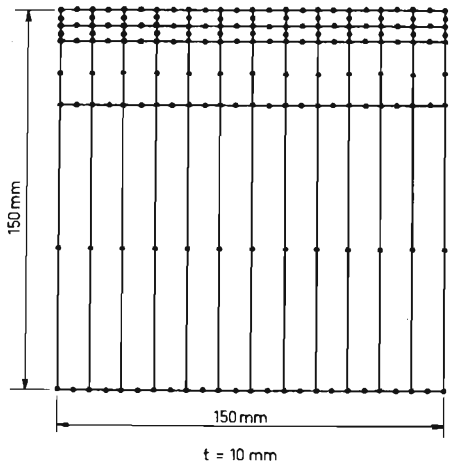

FIGURE 8 : Finite Element Mesh for Plate-Weld Problem

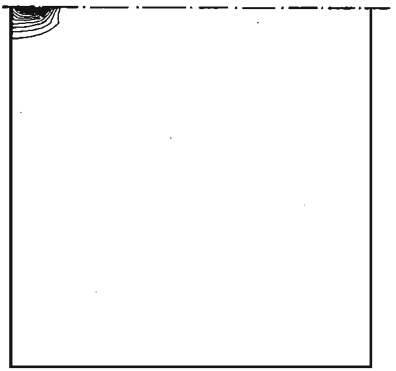

TIME = 6 sec.
TIME INTERVAL = 1

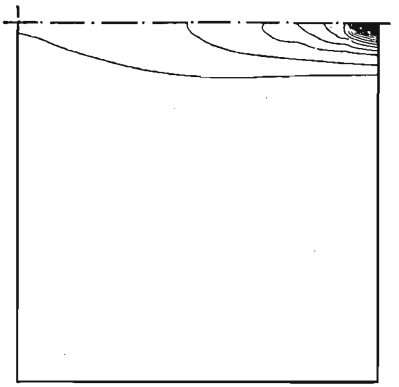

TIME = 75 sec.
TIME INTERVAL = 11

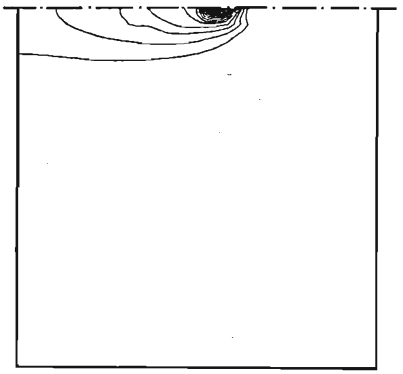

TIME = 44 sec.
TIME INTERVAL = 7

CONTOURS:

MAXIMUM = 1600°C
MINIMUM = 475°C
INCREMENT = 125°C

FIGURE 9 : Temperature Variation in Plate with Time

The results of the analysis are presented in Figs. 10 to 12. In Figs. 10a to 10c, the plastic zones for three of the time intervals are shown together with principal stress plots. Gauss-points that are plastic are shown by a circle and the plastic zones shown by the shaded zones. The final residual stress pattern that remains after the plate has cooled is shown in Fig. 10d. In Fig. 11 the variation of the longitudinal residual stresses which remain after the plate has finally cooled completely are plotted. These are compared with experimental results for the same problem given in Ref. 11. Good agreement is observed between the present analysis and these experimental results. Finally in Fig. 12, displacement plots (magnified 25 times) show the plate distortion produced by the welding.

5. CONCLUSION

It has been shown that the constant stiffness, initial force method in the Finite Element Method may be used successfully to analyse thermal stress problems even when highly non-linear material behaviour is encountered. The proposed solution algorithm has proved to be stable even in the extreme welding problem where material strength decreases to zero in the region near the heat source.

The consideration of all possible material non-linearities such as variable elasticity, plasticity and creep is limited only by the amount of tension test data available for high temperatures and the subsequent representation of such data by smooth functions that can be generated for the computer solution.

The analysis for thermal distortion and residual stresses has many applications in design: for example, their effects on stability of compression panels. In addition such analyses should provide information to plan welding procedures to minimize distortion and also for the determination of pre-heat necessary to reduce residual stresses to a minimum.

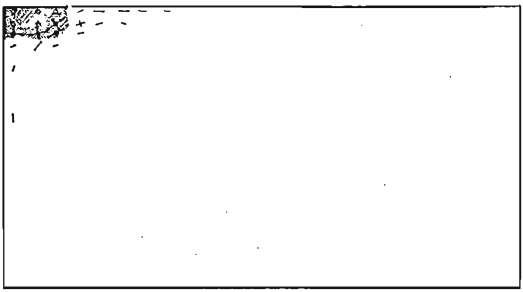

(a) Plastic Zone in Plate Time t = 1

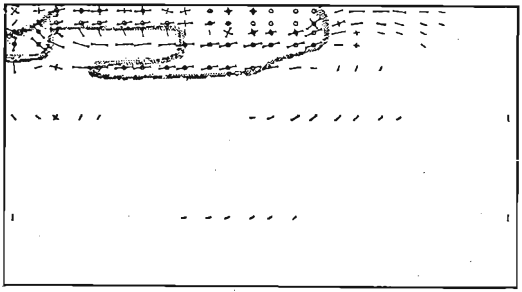

(b) Plastic Zone in Plate Time t = 7

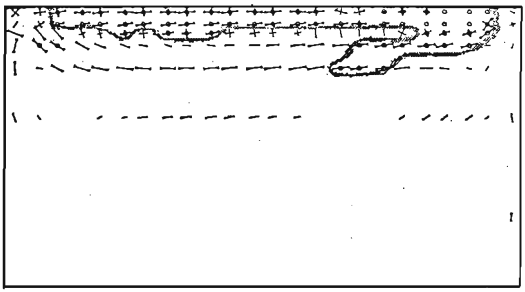

(c) Plastic Zone in Plate Time t = 11

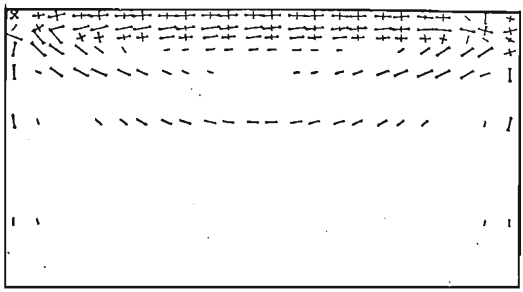

(d) Residual Principal Stresses in Plate

FIGURE 10 : Plastic Zone and Residual Principal Stress

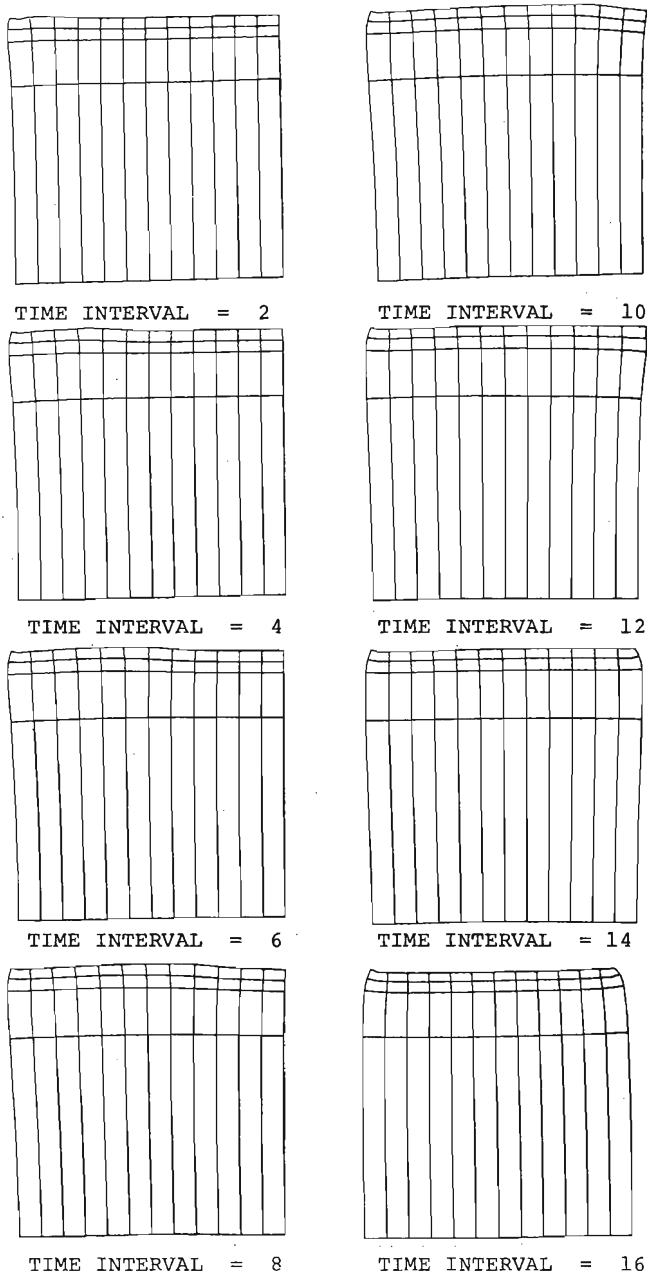

FIGURE 11 : Deformations of Plate with Time

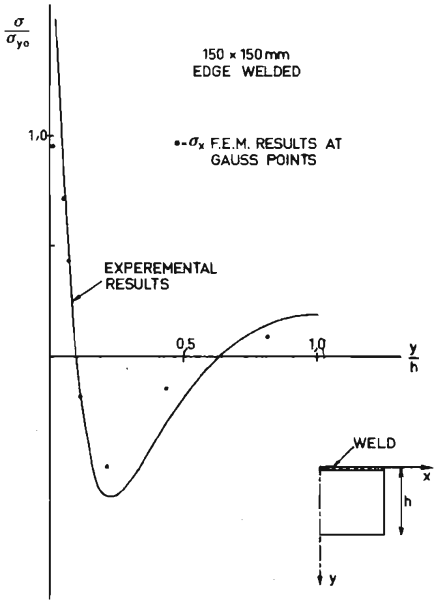

FIGURE 12 : Comparison of Theory with Measured Stress Values

APPENDIX A - INCREMENTAL CORRECTION METHOD

The incremental relationships Equations 25 and 29 are only valid for small values of $\Delta\bar{\varepsilon}_p$, since the direction vector $\{S\}$ and the strain hardening parameter (H) may otherwise change within the interval. Thus Equation 25 must be re-written in incremental form as

$$d\Delta\sigma_p = \{S\}^T [D] \{S\} d\Delta\bar{\varepsilon}_p \tag{54}$$

Thence for a finite increment,

$$\Delta\bar{\sigma}_p = \int_0^{\Delta\bar{\varepsilon}_p} \{S\}^T [D] \{S\} d\Delta\bar{\varepsilon}_p = \int_0^{\Delta\bar{\varepsilon}_p} C d\Delta\bar{\varepsilon}_p \tag{55}$$

In a similar manner,

$$\Delta\sigma_{yE} = \int_0^{\Delta\bar{\varepsilon}_p} H d\Delta\bar{\varepsilon}_p \tag{56}$$

Equation 31 now becomes an integral equation,

$$\Delta F = \bar{\sigma}_+^* - \sigma_{y(\varepsilon_-, T_+)} = \int_0^{\Delta\bar{\varepsilon}_p} C d\Delta\bar{\varepsilon}_p + \int_0^{\Delta\bar{\varepsilon}_p} H d\Delta\bar{\varepsilon}_p \tag{57}$$

An approximate solution of the integral equation can be obtained by treating Equation 57 as an initial value problem. Starting with the known values of $\{S_o\}$ and H_o at stress level $\{\sigma_+^*\} = \{\sigma_o\}$, the correction to the actual value on the yield surface $\{\sigma_+\} = \{\sigma_m\}$ is performed in m small steps.

The recursion formulas are, for the ith step,

$$\Delta F_i = \frac{\sigma_{i-1} - \sigma_y (\varepsilon_-, T_+)}{m + 1 - i} \tag{58}$$

$$\Delta\bar{\varepsilon}_{p,i} = \frac{\Delta F_i}{C_{i-1} + H_{i-1}}$$

$$\{\sigma\} = \{\sigma_{i-1}\} - [D] \{S_{i-1}\} \Delta\bar{\varepsilon}_{p,i}$$

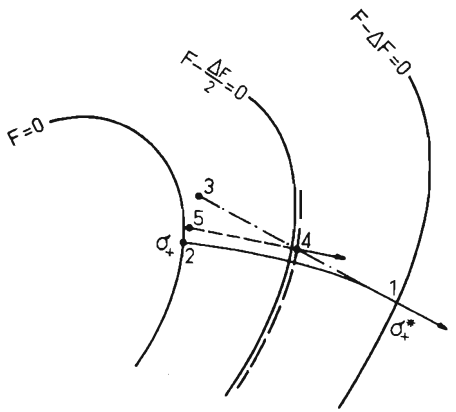

FIGURE 13 : Corrections to Yield Surface

A graphical interpretation of the method in plane stress is shown in Fig. 13 for ideal Von-Mises Plasticity. The correction from σ_+^* to σ_+ is along the curved line 1 - 2. If this correction is performed in one step it would follow the straight line 1 - 3 with the normality vector computed at the fictitious yield surface, $F - \Delta F = 0$. Point 3 is therefore some distance away from the true yield surface. An improved solution is shown using 2 steps. The correction is first made to point 4 where the normality vector is recomputed and hence the final correction 5 is much closer to the yield surface. In practice 10 or more steps can be used to reach a point very close to the yield surface.

APPENDIX B - NOMENCLATURE

Symbol	Meaning
$A(T,\varepsilon)$	function of yield surface with temperature
B	strain transformation matrix
C	matrix scalar, relating equivalent plastic stress and strain
D	constitutive matrix for the material
D_+, D_-	constitutive matrix at beginning and end of time steps
e_x, e_y, e_z	direct deviatoric strain components
ΔF_o	load increment vector
$F(\bar{\sigma}_p, \bar{\varepsilon}_p, T)$	yield function
$H(T,\varepsilon)$	function of yield surface with strain
K	element stiffness matrix
K_o, K	structure stiffness matrices (initial, and at some time interval)
ΔK	increment in K
ΔR_i	residual force vector
s_x, s_y, s_z	direct deviatoric stress components
S	deviatonic stress vector
T, dT	temperature, variation in temperature
α_T	coefficient of thermal expansion
α	over relaxation factor
$\gamma_{xy}, \gamma_{yz}, \gamma_{zx}$	shear strain components
$\tau_{xy}, \tau_{yz}, \tau_{zx}$	shear stress components
$\bar{\varepsilon}_p$	equivalent plastic strain
$\Delta\varepsilon_e$	elastic strains
$\Delta\varepsilon_{\Delta E}$	increment in elastic strain
$\Delta\bar{\varepsilon}_c$	equivalent creep strain
$\bar{\sigma}$	equivalent stress
$\Delta\sigma$	stress increment
σ_y	yield stress
σ_D	stress matrix used for calculating $\bar{\sigma}$

Symbol	Meaning
$\Delta\bar{\sigma}_p$	elastic over stress
σ	stress matrix
$\Delta\varepsilon_T$	thermal strain increment
$\Delta\varepsilon_o$	initial strain vector
$\varepsilon_+, \varepsilon_-$	strains at end and beginning of interval
$\varepsilon_p, \Delta\varepsilon_p$	plastic strain vector, increment in plastic strain
$\Delta\delta$	increment in nodal displacements
σ_-, σ_+	stresses at beginning and end of interval

APPENDIX C - REFERENCES

1. DWIGHT, J.B., "Collapse of Steel Compression Panels", Proc. Conf. Developments in Bridge Design and Construction, Crosby Lockwood, London, 1971.

2. BEER, G., MEEK, J.L. "Transient Heat Flow in Solids", Int. Conference Finite Element Methods in Engineering, Sydney, 1974.

3. BEER, G."Elasto-Plastic Thermal Stress Analysis", Ph.D. Dissertation, University of Queensland, Australia, 1975.

4. YAMADA, Y., IWATA, K. "Finite Element Analysis of Thermo-Viscoelastic Problems", Seisau - Kenkyu, Vol. 24, No. 4, 1972.

5. NAYAK, G.C., ZIENKIEWICZ, O.C. "Elasto-Plastic Stress Analysis - A Generalization for Various Constitutive Relations including Strain Softening". Int. Journal Numerical Methods. Eng., Vol. 5, 113-135, 1972.

6. ARGYRIS, J.H. "Finite Element Analysis of Thermo-Mechanical Problems", Conf. Matrix Methods Structural Mechanics, Wright-Patterson Air Force Base, Ohio, 1972.

7. IRONS, B.M. "A Frontal Solution Program for Finite Element Analysis", Int. Journal Num. Methods in Eng., Vol. 2, 5-32, 1970.

8. Seminar on the Performance of Steel in Fires, B.H.P. Melbourne Research Labs., Melbourne, Australia, 1972.

9. RADAJ, D. "Berechnung Der Schweisseigensspannungen in Stäben mit Längsnähten", Schweissen und Schneiden, Vol. 2, No. 7, 1971.

10. BENHAM. "Thermal Stress", Pitman & Sons, 1964.

11. RAO, N.R.N., ESTUAR, F.R., TALL, L. "Residual Stresses in Welded Shapes", Welding Journal (U.S.A.), Vol. 43, No. 7, July 1964.

12. SKINNER, D.H. "The Measurement of High Temperature Properties of Steel", B.H.P. Melbourne Research Lab. Report No. 18/8, 1972, Melbourne, Australia.

CIVIL ENGINEERING RESEARCH REPORTS

CE No.	Title	Author(s)	Date
1	Flood Frequency Analysis: Logistic Method for Incorporating Probable Maximum Flood	BRADY, D.K.	February, 1979
2	Adjustment of Phreatic Line in Seepage Analysis by Finite Element Method	ISAACS, L.T.	March, 1979
3	Creep Buckling of Reinforced Concrete Columns	BEHAN, J.E. & O'CONNOR, C.	April, 1979
4	Buckling Properties of Monosymmetric I-Beams	KITIPORNCHAI, S. & TRAHAIR, N.S.	May, 1979
5	Elasto-Plastic Analysis of Cable Net Structures	MEEK, J.L. & BROWN, P.L.D.	November, 1979
6	A Critical State Soil Model for Cyclic Loading	CARTER, J.P., BROOKER, J.R. & WROTH, C.P.	December, 1979
7	Resistance to Flow in Irregular Channels	KAZEMIPOUR, A.K. & APELT, C.J.	February, 1980
8	An appraisal of the Ontario Equivalent Base Length	O'CONNOR, C.	February, 1980
9	Shape Effects on Resistance to Flow in Smooth Rectangular Channels	KAZEMIPOUR, A.K. & APELT, C.J.	April, 1980
10	The Analysis of Thermal Stress Involving Non-Linear Material Behaviour	BEER, G. & MEEK, J.L.	April, 1980
11	Buckling Approximations for Laterally Continuous Elastic I-Beams	DUX, P.F. & KITIPORNCHAI, S.	April, 1980

CURRENT CIVIL ENGINEERING BULLETINS

4 *Brittle Fracture of Steel — Performance of ND18 and SAA A1 structural steels: C. O'Connor (1964)*

5 *Buckling in Steel Structures — 1. The use of a characteristic imperfect shape and its application to the buckling of an isolated column: C. O'Connor (1965)*

6 *Buckling in Steel Structures — 2. The use of a characteristic imperfect shape in the design of determinate plane trusses against buckling in their plane: C. O'Connor (1965)*

7 *Wave Generated Currents — Some observations made in fixed bed hydraulic models: M.R. Gourlay (1965)*

8 *Brittle Fracture of Steel — 2. Theoretical stress distributions in a partially yielded, non-uniform, polycrystalline material: C. O'Connor (1966)*

9 *Analysis by Computer — Programmes for frame and grid structures: J.L. Meek (1967)*

10 *Force Analysis of Fixed Support Rigid Frames: J.L. Meek and R. Owen (1968)*

11 *Analysis by Computer — Axisymetric solution of elasto-plastic problems by finite element methods: J.L. Meek and G. Carey (1969)*

12 *Ground Water Hydrology: J.R. Watkins (1969)*

13 *Land use prediction in transportation planning: S. Golding and K.B. Davidson (1969)*

14 *Finite Element Methods — Two dimensional seepage with a free surface: L.T. Isaacs (1971)*

15 *Transportation Gravity Models: A.T.C. Philbrick (1971)*

16 *Wave Climate at Moffat Beach: M.R. Gourlay (1973)*

17 *Quantitative Evaluation of Traffic Assignment Methods: C. Lucas and K.B. Davidson (1974)*

18 *Planning and Evaluation of a High Speed Brisbane-Gold Coast Rail Link: K.B. Davidson, et al. (1974)*

19 *Brisbane Airport Development Floodway Studies: C.J. Apelt (1977)*

20 *Numbers of Engineering Graduates in Queensland: C. O'Connor (1977)*